Int J Cardiovasc Imaging (2012) 28:153–162
DOI 10.1007/s10554-010-9760-7

ORIGINAL PAPER

# Prospectively versus retrospectively ECG-gated 256-slice coronary CT angiography: image quality and radiation dose over expanded heart rates

**Yang Hou · Yong Yue · Wenli Guo · Guoqiang Feng · Tao Yu · Guangwei Li · Mani Vembar · Mark E. Olszewski · Qiyong Guo**

Received: 24 May 2010 / Accepted: 26 November 2010 / Published online: 14 December 2010


**Abstract** To compare image quality and radiation dose estimates for coronary computed tomography angiography (CCTA) obtained with a prospectively gated transaxial (PGT) CT technique and a retrospectively gated helical (RGH) CT technique using a 256-slice multidetector CT (MDCT) scanner and establish an upper limit of heart rate to achieve reliable diagnostic image quality using PGT. 200 patients (135 males, 65 females) with suspected coronary artery disease (CAD) underwent CCTA on a 256-slice MDCT scanner. The PGT patients were enrolled prospectively from January to June, 2009. For each PGT patient, we found the paired ones in retrospective-gating patients database and randomly selected one patient in these match cases and built up the RGH group. Image quality for all coronary segments was assessed and compared between the two groups using a 4-point scale (1: non-diagnostic; 4: excellent). Effective radiation doses were also compared. The average heart rate ± standard deviation (HR ± SD) between the two groups was not significantly different (PGT: 64.6 ± 12.9 bpm, range 45–97 bpm; RGH: 66.7 ± 10.9 bpm, range 48–97 bpm, $P = 0.22$). A receiver-operating characteristic (ROC) analysis determined a cutoff HR of 75 bpm up to which diagnostic image quality could be achieved using the PGT technique ($P < 0.001$). There were no significant differences in assessable coronary segments between the two groups for HR ≤ 75 bpm (PGT: 99.9% [961 of 962 segments]; RGH: 99.8% [1038 of 1040 segments]; $P = 1.0$). At HR > 75 bpm, the performance of the PGT technique was affected, resulting in a moderate reduction of percentage assessable coronary segments using this approach (PGT: 95.5% [323 of 338 segments]; RGH: 98.5% [261 of 265 segments]; $P = 0.04$). The mean estimated effective radiation dose for the PGT group was 3.0 ± 0.7 mSv, representing reduction of 73% compared to that of the RGH group (11.1 ± 1.6 mSv) ($P < 0.001$). Prospectively-gated axial coronary computed tomography using a 256-slice multidetector CT scanner with a 270 ms tube rotation time enables a significant reduction in effective radiation dose while simultaneously providing image quality comparable to the retrospectively gated helical technique. Our experience demonstrates the applicability of this technique over a wider range of heart rates (up to 75 bpm) than previously reported.

**Keywords** Coronary CT angiography · Radiation dose · Prospective gating · Image quality

Y. Hou · Y. Yue · W. Guo · G. Feng · T. Yu · G. Li · Q. Guo (✉)
Department of Radiology, Shengjing Hospital of China, Medical University, 36 Sanhao Street, 110004 Shenyang, Liaoning Province, People's Republic of China
e-mail: houy2@sj-hospital.org

M. Vembar · M. E. Olszewski
CT Clinical Science, Philips Healthcare, Cleveland, OH 44143, USA

## Introduction

Coronary computed tomography angiography (CCTA) has become the preferred noninvasive method to rule out coronary artery disease (CAD) in intermediate risk, symptomatic patients [1–10]. However, radiation dose concerns associated with retrospectively gated helical (RGH) CCTA techniques limited its application in a larger patient population prior to the introduction of prospectively gated transaxial (PGT) CCTA, which enabled a 63–83% radiation dose reduction. Nonetheless, the application of PGT CCTA with 64-slice and dual-source multidetector computed tomography (MDCT) was limited to patients with heart rates below 65 bpm [11–18].

Newer-generation, wide-coverage MDCT systems have attempted to expand the population of patients eligible for low-dose CCTA. Preliminary investigations using 320-slice MDCT demonstrated PGT CCTA at low heart rates, and explored its use in patients with heart rates above 65 bpm; however, those studies noted an increased radiation dose in this subgroup due to a widened acquisition window [19–21]. Early experience with PGT using a 256-slice MDCT scanner with 8 cm z-axis coverage, a rotation time of 270 ms, and novel radiation dose reduction technologies [22] was also reported [23, 24]. Some of these studies focused on patients with heart rates below 65 bpm due to previously established clinical practice using 64-slice MDCT [23, 24], while others suggest that the increased temporal resolution may enable low-dose PGT at higher heart rates [25]; however, these observations need further investigation. This study aims to compare the image quality and effective radiation dose of PGT with RGH CCTA using 256-slice MDCT, and to determine whether the faster rotation time of the scanner enables low-dose PGT at higher heart rates than previously reported.

## Methods and materials

### Study group

The study population consisted of 200 patients (135 male, 65 female, mean age: 56 ± 10 years) who underwent cardiac CT angiography on a 256-slice MDCT scanner (Brilliance iCT, Philips Healthcare, Cleveland, OH, USA). The PGT patients were enrolled prospectively from January to June, 2009. For each PGT patient, we found the paired ones in RGH patient database. The selection criteria for matching were age (within 2 years), BMI (within 5%), heart rate (2%) and heart rate variability (within 3%). Then we randomly selected patients from this group to match the PGT group.

All patients were referred to cardiac CTA for the rule-out of native coronary artery disease (CAD; PGT group), with those patients additionally needing cardiac functional analysis undergoing RGH. Patients with renal insufficiency (creatinine $\leq$ 120 μmol/l), stents and coronary artery bypass grafts (CABG) were excluded from the study. The study was approved by our medical school Institutional Review Board (IRB). Informed consent, including information about radiation risk from MDCT scans and reactions to iodine was obtained from all patients.

### Patient preparation

Other than pre-medication that may already have been given to the patients, no additional $\beta$-blocker medications were administered upon arrival to further lower heart rates. In addition, no nitrates were used in this study.

### Data acquisition

#### *Injection protocol*

The examination included a low-dose scout image (Surview), followed by a coronary calcium scoring scan using prospective ECG gating. The images from the calcium scoring scan were used to optimize the scan length needed for the diagnostic CCTA scans (both RGH and PGT). The scan coverage was planned from the level of 1 cm below the tracheal bifurcation to the diaphragm. A volume of 70–80 ml of contrast media (Iohexol 350; GE Healthcare, Shanghai, China) followed by 40 ml of saline was injected into the antecubital vein at a rate of 5–6 ml/s with an 18-gauge catheter using a dual-head injector (Ulrich REF XD 2051; Ulrich Medical GmbH, Ulm Germany). Automatic bolus tracking (Bolus Pro, Philips Healthcare, Cleveland, OH, USA) was used by defining a region of interest (ROI) in the ascending aorta at the level of aorto-pulmonary

fenestration, with the scans initiated 6 s after the signal attenuation reached a pre-determined threshold of 180 Hounsfield Units (HU).

*Acquisition protocol: retrospectively gated helical (RGH) scans*

RGH scans were acquired with a tube voltage of 120–140 kVp (140 kVp was used in two patients whose BMI > 30), 0.27 ms rotation time, an effective tube current–rotation time product (normalized to the pitch factor) of 800–1,000 mAs, a pitch factor of 0.16 and a fixed detector collimation of 128 × 0.625 mm. The standard temporal resolution of 135 ms is further improved by employing advanced cardiac adaptive multi-cycle reconstruction algorithms that combine data from consecutive cardiac cycles [26]. The use of the overlapped pitch, along with dedicated cardiac gating algorithms (Beat-to-Beat Variable Delay Algorithm, Philips Healthcare, Cleveland, OH, USA) [27, 28] enable the detection and reconstruction of the quiescent physiologic cardiac phase of interest—typically ventricular diastole or diastasis at lower heart rates or the end-systolic rest phase at higher heart rates [25]. Since left ventricular functional assessment had to be performed in this sub-group of patients and we wanted to retain the option of reconstructing any cardiac phase for coronary image quality assessment, ECG tube current modulation was turned off. However, other dose reduction technologies, such as dynamic helical z-collimation (Eclipse DoseRight Collimator, Philips Healthcare, Cleveland, OH, USA) that reduces the excess radiation exposure caused by z-overscanning occurring at the beginning and the end of helical scans were employed. This dynamic collimator has been shown to reduce radiation exposure in RGH scans by approximately 25% for typical cardiac scan lengths [22].

*Acquisition protocol: prospectively gated transaxial (PGT) scans*

These are axial scans prospectively triggered only during a particular physiologic cardiac phase of interest [11]. PGT scans were acquired with a tube voltage of 120–140 kVp (140 kVp was used in two patients whose BMI > 30), 270 ms rotation time, and an effective tube current–X-ray on time product of 210–330 mAs. The scanner comes equipped with an adaptive axial z-collimation that optimizes the craniocaudal scan length for each patient [22]. Also, a field-of-view (FOV) dependent z-increment, or step size, dynamically reduces overlap between steps (i.e., increases step size) with reduced FOV [29]. Scans were prospectively triggered at the center of a physiologic rest phase for each patient. This trigger typically occurred at 75% of the R-R interval (corresponding to diastasis) for heart rates <70 bpm and 45% of the R-R interval (end-systolic rest phase) for heart rates ≥70 bpm. An additional phase tolerance of 5% around a specific phase of interest was employed for heart rates ≥70 bpm prior to the scan. No phase tolerance was used in patients with heart rates <70 bpm. In addition, real-time arrhythmia handling capabilities enable disabling the x-rays until the heart rate stabilizes, thus providing dose savings by scanning only during sinus rhythm. The standard temporal resolution is 135 ms—multi-cycle reconstructions are not available in this mode.

Table 1 shows a summary of acquisition parameters in both protocols used in this study.

**Table 1** Summary of the acquisition protocols used in the study

| Parameters | Prospective (PGT) | Prospective (PGT) |
|---|---|---|
| Tube voltage (kVp) | 120–140 | 120–140 |
| Current–time product (mAs)[a] | 210–340 | 800–1,000 |
| Rotation time (ms) | 270 | 270 |
| Pitch | NA | 0.16 |
| Acquisition angle (degrees)[b] | 280–480° | – |
| Detector configuration (mm) | 128 × 0.625[c] | 128 × 0.625 |
| Field-of-view (FOV, mm) | 250 | 250 |
| Threshold for bolus tracking (HU) | 180 | 180 |
| Post-threshold delay (sec) | 6 | 6 |
| Slice thickness (mm) | 0.9 | 0.9 |
| Increment (mm) | 0.45 | 0.45 |

[a] mAs in PGT: mA × X-ray ON time. mAs (eff) in RGH: (mA × rotation time)/pitch

[b] The values of the acquisition angle in PGT depend on the use of phase tolerance

[c] Adaptive axial z-collimation is used to optimize the craniocaudal scan length

### Image reconstruction and analysis

All images were reconstructed using a standard reconstruction kernel (XCB) with a thickness of 0.9 mm and an increment of 0.45 mm and at a FOV of 250 mm. From the RGH scans, images were reconstructed at multiple physiologic cardiac phases and the phase with the best image quality was used for assessment. From the PGT scans, images from only the phase(s) scanned (75% of the R-R interval at heart rates <70 bpm and 45% of the R-R interval with 5% phase tolerance at heart rates ≥70 bpm) were reconstructed.

All images were then transferred to a workstation (Brilliance Workspace V4.02, Philips Healthcare, Cleveland, OH, USA), with analysis performed with both standard formats (axial, multiplanar reformations [MPR], and curved multiplanar reformations [CMPR]) and also with a dedicated cardiac application (Comprehensive Cardiac Analysis [CCA]). For analysis, the coronary arteries were segmented into a 15-segment American Heart Association (AHA) model [30] and segments with a luminal diameter of ≥1.5 mm were ranked using a 4-point scale (4: excellent image quality, vessels with sharp edges without discontinuity and artifacts; 3: good image quality, vessels with mild artifacts without discontinuity and could be evaluated; 2: fair, vessels with moderate artifacts, blurring without discontinuity and difficult to evaluate; 1: poor, with severe motion artifacts, discontinuity and non-assessable). Segments with score of ≥3 were considered assessable. Images were evaluated in consensus by two experienced radiologists (with more than 5 years experience in CCTA) side-by-side who were blinded to the mode of acquisition.

Objective image quality parameters were measured. CT image attenuation in Hounsfield Units (HU) and image noise were measured in a region of interest (ROI) of 1 $cm^2$ in the ascending aorta at the level of the origin of the left main coronary artery on the axial images. The image noise was measured as the standard deviation of HU within each ROI.

### Radiation dose measurements

The volume computed tomography dose index ($CTDI_{vol}$) and the dose-length product (DLP) were noted from the CT console after each scan. The estimated effective radiation dose was derived as the product of the DLP and a conversion coefficient $k$, where $k$ is the conversion coefficient for the chest ($k = 0.014$ mSv $mGy^{-1}$ $cm^{-1}$) [31, 32].

### Statistical analysis

Statistical analyses were performed by using commercially available software (SPSS 11.5, SPSS, Chicago, IL, USA). Continuous variables were expressed as mean ± standard deviation, with categorical variables expressed as frequencies or percentages. Continuous variables and demographic data were compared by a Student's t-test. A receiver-operating characteristic (ROC) analysis was performed to establish an upper threshold of heart rate for the prediction of motion artifacts and consistent diagnostic image quality. Point estimates, 95% confidence intervals (CIs) and area under the curve (AUC) were calculated. The optimum threshold of heart rate ($HR_{thresh}$) for the prediction of motion artifacts in PGT scans was chosen. Each scan group (PGT and RGH) was sub-divided into low heart rate (≤$HR_{thresh}$) and high heart rate (>$HR_{thresh}$) subgroups. Chi-square test or Fisher's exact test was used to compare the proportion of assessable segments (score ≥ 3) between PGT and RGH protocol when appropriate. A $P$ value $< 0.05$ was considered statistically significant.

## Results

All patients underwent CCTA successfully. Statistical analysis showed the gender, age, body mass index (BMI) and heart rate matched between the two groups. Table 2 summarizes the demographic data and scan details (scan length and scan time) of the two cohorts ($P > 0.05$ for both).

### Coronary image quality comparisons

1,300 segments with diameter ≥1.5 mm were available for analysis in the PGT group. Image quality was considered assessable in 1,284 (98.8%) segments with score ≥3. Median subjective image quality for all segments was 4. Out of the 1,305 segments with diameter ≥1.5 mm analyzed in the RGH group, image quality was considered assessable in 1,299

**Table 2** Summary of demographic and scan details of the two groups

| Patient/Scan details | Prospective scans (PGT, N = 100) | Retrospective scans (RGH, N = 100) | *P* |
|---|---|---|---|
| Age (years) | 57.3 ± 10.3 | 55.3 ± 10.7 | 0.21 |
| Gender (male/female) | 65/35 | 70/30 | |
| Body mass index (BMI) | 26.7 ± 5.3 (20–32) | 25.8 ± 7.4 (19–34) | 0.19 |
| Heart rate (bpm) | 64.6 ± 12.9 (45–97) | 66.7 ± 10.9 (48–97) | 0.22 |
| Heart rate variation (HRV, bpm) | 2.1 ± 1.1 (0–16) | 2.4 ± 2.2 (0.5–11.9) | 0.20 |
| Scan length (cm) | 11.1 ± 1.1 (9.4–12.8) | 11.4 ± 1.0 (8.8–13.2) | 0.10 |
| Scan time (s) | 4.6 ± 0.3 (3.7–7.4) | 4.3 ± 0.4 (4.3–6.5) | 0.09 |

With the exception of gender, all data are shown as mean ± standard deviation, along with the range

(99.5%) segments. Median subjective image quality for all segments was 4. There were significant differences in assessable coronary segments between the two groups ($P = 0.03$).

A receiver-operating characteristic (ROC) analysis determined an upper threshold of heart rate of 75 bpm beyond which artifacts resulting from coronary motion started affecting the image quality in the PGT group (AUC = 0.92; 95% CI: 0.87, 0.98; $P < 0.05$; see Fig. 1). For heart rates ≤75 bpm there were no significant differences in assessable coronary segments between the two groups (PGT: 99.9% [961 of 962 segments]; RGH: 99.8% [1,038 of 1,040 segments]; $P = 1.0$). The median image quality for both PGT and RGH at heart rates ≤75 bpm was 4. At heart rates >75 bpm, the performance of the PGT technique was influenced by motion artifacts, resulting in a moderate reduction of assessable coronary segments using this approach (PGT: 95.5% [323 of 338 segments]; RGH: 98.5% [261 of 265 segments]; $P = 0.04$). Despite the increase in the number of non-diagnostic segments, the median image quality for both PGT and RGH at heart rates >75 bpm was 4. Table 3 summarizes the image quality characteristics of the two patient groups.

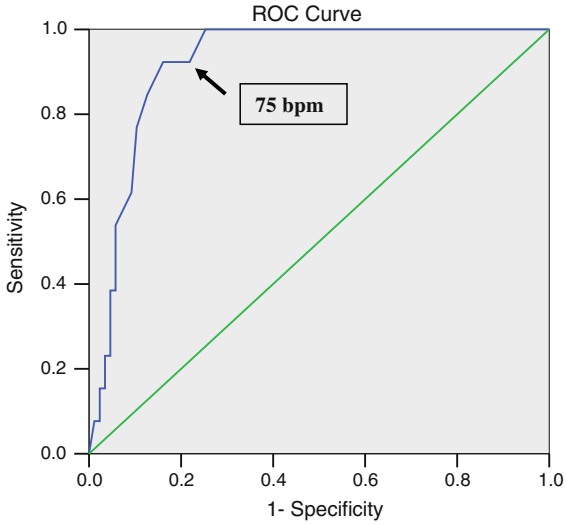


**Fig. 1** Receiver-operator characteristic (*ROC*) curve to establish a cut off mean heart rate value up to which diagnostic image quality can be consistently achieved using PGT. The curve suggests a cut off of 75 bpm beyond which coronary image quality was affected (Area under curve [*AUC*] = 0.92; 95% CI: 0.87, 0.98; $P < 0.05$)

Based on the heart rate of 75 bpm identified in the ROC analysis, a patient-based analysis showed that 73 of 74 subjects (98.9%) in the PGT group and 78 of 80 subjects (97.5%) in the RGH group, respectively, had diagnostic image quality. Thus there is no statistically significant difference between the groups based on this heart rate threshold ($P = 1.0$). At heart rates >75 bpm,14 of 26 subjects (53.9%) in the PGT group and 17 of 20 subjects (85%) in the RGH group, respectively, had diagnostic image quality. There is statistically significant difference between two groups ($P = 0.03$) above the heart rate threshold. Figures 2 and 3 are representative examples of cases scanned with PGT, with average heart rates of 54 bpm and 92 bpm respectively, both ranked 4. Figure 4 is a clinical example showing the real-time arrhythmia handling capabilities of the PGT mode where the scan was paused (and x-rays turned off) during an arrhythmic event and resumed once sinus rhythm was restored—the image quality was not affected by the premature beat and the coronary image quality was ranked 4.

The objective image quality measurements are summarized in Table 4. No significant differences were seen in the mean CT attenuation and noise

**Table 3** Comparison of coronary image quality between PGT and RGH groups

| Heart rate | Scan type | N | Mean HR (bpm) | Assessable segments (%) | *P* |
|---|---|---|---|---|---|
| All | PGT | 100 | 64.6 ± 12.9 | 98.8% (1,284/1,300) | 0.03[a] |
| | RGH | 100 | 66.7 ± 10.9 | 99.5% (1,299/1,305) | |
| ≤75 bpm | PGT | 74 | 58 ± 7.5 (range 45–75) | 99.9% (961/962) | 1.0[b] |
| | RGH | 80 | 61 ± 7.1 (range 48–75) | 99.8% (1,038/1,040) | |
| >75 bpm | PGT | 26 | 84 ± 7.1 (range 76–97) | 95.5% (323/338) | 0.04[a] |
| | RGH | 20 | 85 ± 6.7 (range 76–97) | 98.5% (261/265) | |

[a] $X^2$ test was used

[b] Fisher's Exact test was used

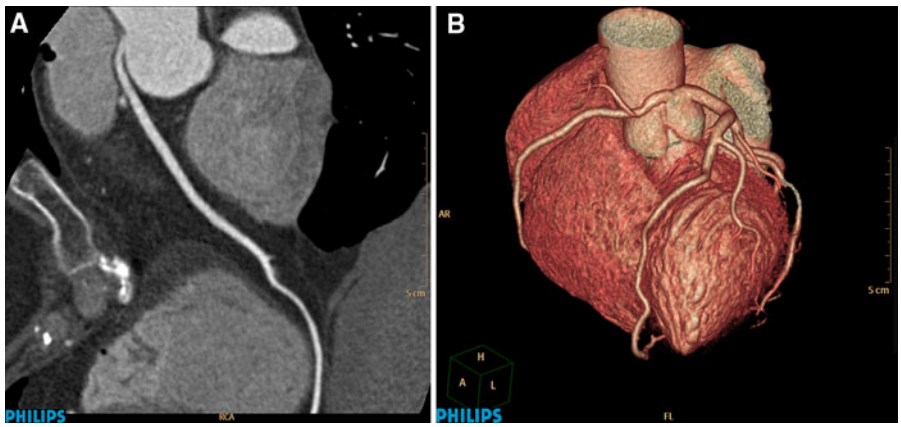


**Fig. 2** PGT-CCTA of a 55 year old female (BMI: 25 and mean HR: 56 ± 1.0 bpm) with an anomalous origin of the right coronary artery (*RCA*). **a** Curved multi-planar reformation (*CMPR*) of the right coronary artery (*RCA*) artery. **b** Volume rendered depiction showing coronary artery system with the anomalous origin of the RCA. The scan was centered at 75% physiologic cardiac phase. All segments were ranked 4 (excellent). Effective dose: 2.3 mSv

(standard deviation) measurements from the two scan groups ($P = 0.87$ and 0.29 for CT attenuation and standard deviation respectively).

### Comparison of radiation dose estimates

There were significant differences in the $CTDI_{vol}$, DLP, and estimated effective radiation dose between the two scan groups ($P < 0.001$; see Table 5). The mean estimated effective radiation dose of the PGT group was 3.0 ± 0.7 mSv, reflecting a reduction of 73% compared to the RGT scans (11.1 ± 1.6 mSv) performed with no dose modulation.

## Discussion

We compared the image quality and radiation dose of PGT and RGH CCTA on a wide-detector, 256-slice MDCT scanner with a gantry rotation time of 270 ms. A recent study using this scanner reported equivalent coronary image quality and a radiation dose reduction of 76% with PGT compared to RGH in 25 patients [23]. Klass, et al., demonstrated significant improvements in image quality and robustness with PGT CCTA on the same scanner when compared to a matched cohort of patients scanned using 64-slice MDCT with the same scan technique and equivalent effective radiation dose [24]. The authors reported 1% non-assessable segments on 256-slice MDCT compared to 5% non-assessable segments on 64-slice MDCT, with the improvement attributed to the faster gantry rotation time of the 256-slice CT [24]. However, as with prior studies [12–18], these investigations focused on lower heart rates, with a mean heart rate of 56 bpm reported during the CCTA acquisitions.

We have shown that PGT using 256-slice MDCT with 270 ms rotation time results in significant

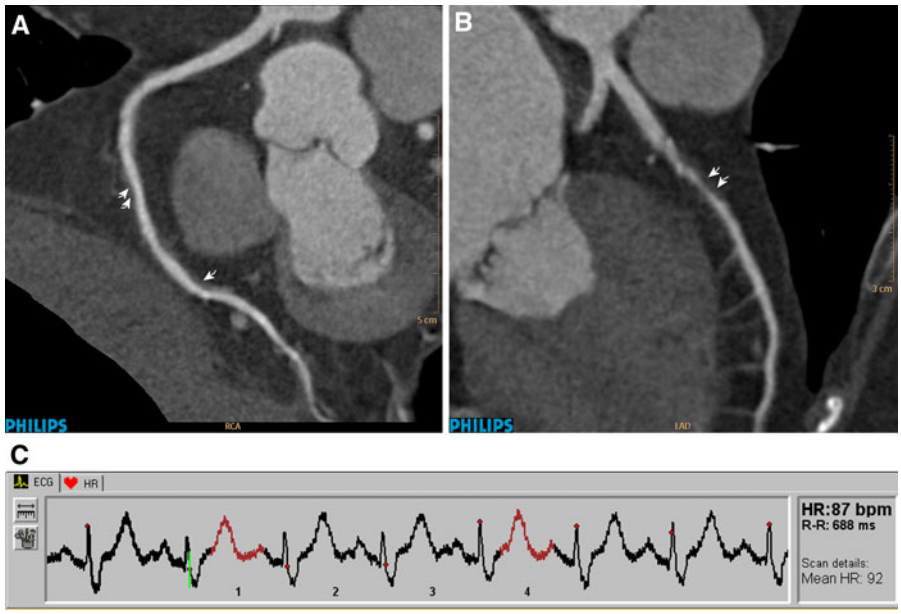


**Fig. 3** PGT-CCTA of a 65 year old female (with BMI: 25 and mean HR: 92 ± 1.2 bpm). **a** Curved multi-planar reformation (*CMPR*) of the RCA showing luminal irregularities (*arrows*). **b** Curved multi-planar reformation of the left anterior descending (*LAD*) artery showing a significant non-calcified lesion (*arrow*). **c** The corresponding ECG. The scan was centered at 45% physiologic cardiac phase, with an additional 5% phase tolerance employed. Effective radiation dose: 3.2 mSv

effective radiation dose reduction and maintained image quality compared to RGH in demographic-, HR-, and BMI-matched patient groups. The percentage of assessable coronary segments was high at 98.8% (PGT) and 99.5% (RGH). The mean heart rates in the PGT group were higher (64.6 ± 12.9 bpm) and the heart rate range was wider (45–97 bpm) than reported in previous studies. The low number of non-assessable segments in this study, despite a higher heart rate range, may be explained by the faster gantry rotation time and increased coverage of the system used. ROC analysis (Fig. 1) suggested a heart rate cut-off of 75 bpm below which there were no significant differences in image quality between PGT and RGH, with negligible non-diagnostic coronary segments (PGT: 0.1%, RGH: 0.2%, $P = 1.0$). This demonstrates an increase in the patient population eligible for PGT compared to prior reports that have established cutoffs of 63 bpm [14] and 59.9 bpm [18] for PGT using 64-slice or dual-source MDCT.

Beyond the heart rate threshold of 75 bpm the difference of image quality between two groups was significant. There was a moderate increase of non-assessable segments using this technique (5%) compared to RGH (1.5%; $p = 0.04$). Fourteen of the 26 patients (53.9%) had diagnostic images in PGT group. This can be explained by the impact of heart rate variations on the cardiac physiology. The increase in heart rate causes an exponential reduction of the duration of ventricular diastasis typically targeted for coronary CTA imaging, making this rest phase disappear at heart rates >80 bpm [33–36]. In contrast, the duration of the composite end-systolic rest period, although not as wide as diastasis, is affected to a lesser extent and is known to range between 100 and 150 ms depending on the heart rate. Recent evidence suggests that it is possible to target this rest period on the 256-slice CT with a standard temporal resolution of 135 ms for heart rates greater than 75 bpm using RGH [37] or PGT [25]. However, because of its narrower window, challenges remain with PGT for patients with high heart rates (as reflected by our patient-based results). While multi-cycle reconstructions benefit RGH [26], these benefits do not extend to PGT. Lastly, rapid changes of heart rate after contrast injection can lead to an error of the prospective triggering time. Despite this, the proportion of assessable segments at heart rates above 75 bpm remained comparable to the proportion of assessable segments reported in previous studies for patients with steady heart rates below 65 bpm [14, 18].

The wide coverage of 256-slice MDCT allowed us to complete PGT scans in less than 5 s, with one to two steps needed to cover the cardiac anatomy. This is in comparison to up to 15.4 s and four to six steps needed on 64-slice and dual-source MDCT [2, 12], thus also minimizing the effects of heart rate variation during the scan.

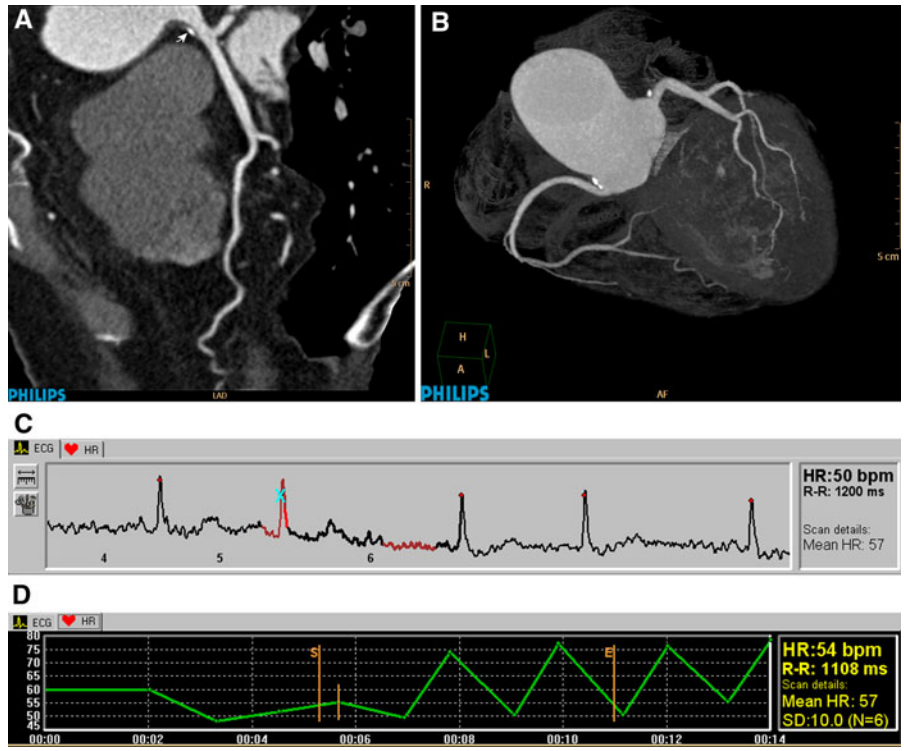


**Fig. 4** PGT-CCTA of a 75 year old female (BMI: 25, mean HR: 57 ± 10.0 bpm and HR variation of 50–78 bpm during the scan). **a** Curved multi-planar reformation (*CMPR*) of the left anterior descending artery (*LAD*) showing a focal calcified lesion at the origin of the left main (*LM*) (*arrow*). **b** A three-dimensional angio-like maximum intensity projection (*MIP*) view showing the coronary artery system. **c** The ECG of the exam and **d** the heart rate variation during the scan. The real-time arrhythmia handling mechanism detected the occurrence of an atrial premature beat—the scan was momentarily suspended (shown as a *light blue* 'X' in **c**) and resumed once sinus rhythm returned, thus not compromising the overall image quality. Effective radiation dose: 4.4 mSv

**Table 4** Objective image quality measurement comparison between PGT and RGH groups

| Objective image quality measurements | Prospective (PGT) | Retrospective (RGH) | *P* |
|---|---|---|---|
| CT attenuation in ascending aorta (HU) | 373.3 ± 68.5 (258.3–444.8) | 371.7 ± 61.7 (243.0–479.0) | 0.87 |
| Image noise (HU) | 33.4 ± 6.3 (19.1–49.6) | 32.2 ± 9.4 (18.7–45.1) | 0.29 |

*HU* Hounsfield unit

**Table 5** Comparison of radiation dose estimates between PGT and RGH groups

| Radiation dose parameters | Prospective (PGT) | Retrospective (RGH) | *t* value | *P* |
|---|---|---|---|---|
| CTDI (mGy) | 19.6 ± 4.4 (16.3–30.2) | 64.7 ± 8.3 (51.0–114.0) | 47.61 | < 0.001 |
| DLP (mGy cm) | 217.1 ± 51.3 (145.7–338.9) | 730.3 ± 105.0 (516.4–1,308.7) | 43.69 | < 0.001 |
| ED (mSv) | 3.0 ± 0.7 (2.0–4.7) | 11.1 ± 1.6 (7.2–18.3) | 45.01 | < 0.001 |

*CTDI* computed tomography dose index, *DLP* dose length product, *ED* effective dose

In addition to demonstrating maintained image quality between PGT and RGH, this study has documented a 73% radiation dose reduction with PGT compared to RGH. The mean effective radiation dose for the PGT group (3.0 mSv) is within the 2.1–6.2 mSv reported previously [12–18]. This

reduction enables CCTA to be performed at an effective radiation dose below that of an invasive coronary angiogram [9, 10]. The extra 5% phase tolerance employed in PGT scans at heart rates greater than 75 bpm resulted in an increase in the average effective radiation dose to 4.0 mSv, which is still within the previously reported range associated with PGT [12–18], and also provided the flexibility of additional reconstruction windows.

Our study has demonstrated the capability of 256-slice, low-dose, PGT CCTA in providing consistent image quality comparable to the traditional RGH technique while also offering significant reduction in effective radiation dose. Our initial experience shows applicability of this technique beyond the commonly recommended heart rates. However, appropriate patient selection, preparation and strict inclusion criteria still hold the key to the consistency and success of the exam. Further studies are needed to evaluate the performance of these new CT systems in providing consistent low dose coronary imaging at higher heart rates.

## Limitations

We acknowledge the following limitations of this study. This was a single center retrospective study of cardiac CTA scans on a newly installed scanner. The protocols used were for the most part the default settings provided by the manufacturer and were not individually adjusted based on a patient's BMI and weight to further reduce radiation dose; however, care was taken in planning the craniocaudal lengths to reduce the radiation exposure in all patients. The use of 100 kVp was not employed as it was not available at the time of this study—this would have helped achieve additional radiation dose savings in certain groups of patients while also facilitating a reduction in the contrast volumes [14, 18]. The number of patients in the high heart rate group (>75 bpm) was small in both PGT and RGH subgroups. No ECG-triggered tube modulation was employed in RGH mode. Had dose modulation techniques been used, the dose associated with the RGH group would have been lower. Lastly, we did not assess the diagnostic accuracy of CCTA by comparing it to invasive coronary angiography.

## Conclusion

Prospectively gated coronary computed tomography using a wide-coverage 256-slice multidetector CT scanner with a fast tube rotation time enables a significant reduction in radiation dose exposure while at the same time providing image quality comparable to the conventional retrospectively gated helical technique. Our experience demonstrates that the image quality of prospectively gated transaxial coronary CT angiography is comparable to retrospectively gated helical scans in patients with heart rates up to 75 bpm, which is higher than reported with previous-generation MDCT scanners.

**Acknowledgments** This work was supported by two provincial government funds—Innovative Reaserch Team of Liaoning Educational Committee (LT2010105) and Liaoning Doctoral Science Foundation (20071048).

**Conflict of interest** Authors who are not employees of Philips Healthcare (Cleveland, OH, USA) controlled the inclusion of all data and information that might have represented a conflict of interest for the authors who are employees of that company.

## References

1. Leschka S, Alkadhi H, Plass A et al (2005) Accuracy of MSCT coronary angiography with 64-slice technology: first experience. Eur Heart J 26:1482–1487
2. Scheffel H, Alkadhi H, Plass A et al (2006) Accuracy of dual-source CT coronary angiography: first experience in a high pre-test probability population without heart rate control. Eur Radiol 16:2739–2747
3. Leber AW, Johnson T, Becker A et al (2007) Diagnostic accuracy of dual-source multi-slice CT-coronary angiography in patients with an intermediate pretest likelihood for coronary artery disease. Eur Heart J 28:2354–2360
4. Mollet NR, Cademartiri F, van Mieghem CA et al (2005) High-resolution spiral computed tomography coronary angiography in patients referred for diagnostic conventional coronary angiography. Circulation 112:2318–2323
5. Raff GL, Gallagher MJ, O' Neill WW et al (2005) Diagnostic accuracy of noninvasive coronary angiography using 64-slice spiral computed tomography. J Am Coll Cardiol 46:552–557
6. Hausleiter J, Meyer T, Hadamitzky M et al (2006) Radiation dose estimates from cardiac multislice computed tomography in daily practice: impact of different scanning protocols on effective dose estimates. Circulation 113:1305–1310
7. Stolzmann P, Scheffel H, Schertler T et al (2008) Radiation dose estimates in dual-source computed tomography coronary angiography. Eur Radiol 18:592–599

8. Einstein AJ, Henzlova MJ, Rajagopalan S (2007) Estimating risk of cancer associated with radiation exposure from 64-slice computed tomography angiography. JAMA 298:317–323
9. Miller SW, Castronovo FP Jr (1985) Radiation exposure and protection in cardiac catheterization laboratories. Am J Cardiol 55(1):171–176
10. Dewey M, Telge F, Schnapauff D et al (2006) Noninvasive detection of coronary artery stenosis with multislice computed tomography or magnetic resonance imaging. Arch Intern Med 145(6):407–415
11. Hsieh J, Londt L, Vaas M et al. (2006) Step-and-shoot data acquisition and reconstruction for cardiac X-ray computed tomography. Med Phys 33:4236–4248
12. Earls JP, Berman EL, Urban BA et al. (2008) Prospectively gated transverse coronary CT angiography versus retrospectively gated helical technique: improved image quality and reduced radiation dose. Radiology 246:742–753
13. Hein F, Meyer T, Hadamitzky M et al. (2009) Prospective ECG-triggered sequential scan protocol for coronary dual-source CT angiography: initial experience. Int J Cardiovasc Imaging 25(2):231–239
14. Husmann L, Valenta I, Gaemperli O et al (2008) Feasibility of low-dose coronary CT angiography: first experience with prospective ECG-gating. Eur Heart J 29:191–197
15. Shuman WP, Branch KR, May JM et al (2008) Prospective verse retrospective ECG gating for 64-detector CT of the coronary arteries: comparison of image quality and patient radiation dose. Radiology 248:431–437
16. Hirai N, Horiguchi J, Fujioka C et al (2008) Prospective versus retrospective ECG-gated 64-detector coronary CT angiography: assessment of image quality, stenosis, and radiation dose. Radiology 248:424–430
17. Klass O, Jeltsch M, Feuerlein S et al. (2009) Prospectively gated axial CT coronary angiography: preliminary experiences with a novel low-dose technique. Eur Radiol 19(4):829–836
18. Stolzmann P, Leschka S, Scheffel H et al (2008) Dual-source CT in step-and-shoot mode: noninvasive coronary angiography with low radiation dose. Radiology 249:71–80
19. Rybicki FJ, Otero HJ, Steigner ML et al. (2008) Initial evaluation of coronary images from 320-detector row computed tomography. Int J Cardiovasc Imaging 24:535–546
20. Hoe J, Toh KH (2009) First experience with 320-row multidetector CT coronary angiography scanning with prospective electrocardiogram gating to reduce radiation dose. J Cardiovasc Comput Tomogr 3(4):257–261
21. Mori S, Nishzawa K, Kondo C et al. (2007) Effective doses in subjects undergoing computed tomography cardiac imaging with the 256-multislice CT scanner. Eur J Radiol. doi:10.1016/j.ejrad.2007.05.001
22. Walker MJ, Olszewski ME, Desai MY et al. (2009) New radiation dose saving technologies for 256-slice cardiac computed tomography angiography. Intl J Cardiovasc Imaging 25:189–199
23. Efstathopoulos EP, Kelekis NL, Pantos I et al. (2009) Reduction of the estimated radiation dose and associated patient risk with prospective ECG-gated 256-slice CT coronary angiography. Phys Med Biol 54(17):5209–5222
24. Klass O, Walker M, Siebach A et al. (2009) Prospectively gated axial CT coronary angiography: comparison of image quality and effective radiation dose between 64- and 256-slice CT. Eur Rad. doi:10.1007/s00330-009-1652-7
25. Weigold WG, Olszewski ME, Walker MJ (2009) Low-dose prospectively gated 256-slice coronary computed tomographic angiography. Int J Cardiovasc Imaging 25: 217–230
26. Manzke R, Grass M, Nielsen T et al (2003) Adaptive temporal resolution optimization in helical cardiac cone beam CT reconstruction. Med Phys 30(12):3072–3080
27. Vembar M, Garcia MJ, Heuscher DJ et al (2003) A dynamic approach to identifying desired physiological phases for cardiac imaging using multislice spiral CT. Med Phys 30(7):1683–1693
28. Heuscher DJ, Chandra S. Multi-phase cardiac imager. 2003 US Patent 6,510,337
29. Hameed TA, Teague SD, Vembar M et al. (2009) Low radiation dose ECG-gated chest CT angiography on a 256-slice multidetector CT scanner. Intl J Cardiovasc Imaging 25:267–278
30. Austen WG, Edwards JE, Frye RL et al. (1975) A reporting system on patients evaluated for coronary artery disease. Report of the Ad Hoc Committee for Grading of Coronary Artery Disease, Council on cardiovascular Surgery, American Heart Association. Circulation 51(4):5–40 (Suppl)
31. Shrimpton PC (2004) Assessment of patient dose in CT. NRPB-PE/1/2004 National Radiological Protection Board. Available via http://www.msct.eu/CT_Quality_Criteria.htm#Download%20the%202004%20CT%20Quality%20Criteria.
32. McCollough C, Cody D, Edyvean S et al. (2008) The measurement, reporting, and management of radiation dose in CT. Tech. Rep. 96 2008. American Association of Physicists in Medicine, College Park
33. Wiggers CJ (1921) Studies on the consecutive phases of the cardiac cycle. The duration of the consecutive phases of the cardiac cycle and the criteria for their precise determination. Am J Physiol 56:415–438
34. Wiggers CJ (1921) Studies on the consecutive phases of the cardiac cycle. The laws governing the relative durations of ventricular systole and diastole. Am J Physiol 56:439–459
35. Chung CS, Karamanoglu M, Kovacs SJ (2004) Duration of diastole and its phases as a function of heart rate during supine bicycle exercise. Am J Physiol Circ Physiol 287:H2003–H2008. doi:10:1152/ajpheart.00404.2004
36. Wang Y, Vidan E, Bergman GW (1999) Cardiac motion of coronary arteries: variability in the rest period and implications for coronary MR angiography. Radiology 213:751–758
37. Mok GS, Yang CC, Chen LK et al. (2010) Optimal systolic and diastolic image reconstruction windows for coronary 256-slice CT angiography. Acad Radiol 17(11):1386–1393